Data supplement for Kaye et al., Neural Insensitivity to the Effects of Hunger in Women Remitted From Anorexia Nervosa. Am J Psychiatry (doi: 10.1176/appi.ajp.2019.19030261)

Methods

Study Procedures (See Table S1)

The night before the hungry day, subjects did not consume anything besides water after dinner at 5:00 pm, had no breakfast, and were scanned at 9:00 am the next day. The night before the fed day, subjects had dinner at 5:00 pm, a snack at 8:45 pm and then breakfast at 7:00 am before the 9:00 am scan. Subjects were given choices from the University of California San Diego (UCSD) Clinical & Translational Research Institute (CTRI) menu but their caloric intake was adjusted to receive 30 cal/kg of body weight/day, with macronutrients distributed as 53% carbohydrate, 32% fat, 15% protein (1). Meals were prepared by the CTRI kitchen and supervised by the CTRI dietitian and staff. CTRI staff recorded participants' food and fluid intake. Water was provided ad lib, but amount consumed was recorded. During the fed cycle (from lunch on Day 2 to 9:00 am on Day 3, or from lunch on Day 3 to 9:00 am on Day 4), the caloric intake was proportioned between 3 meals and 2 snacks. Subjects had 24% of their calories at lunch, 8% of their calories at the mid-afternoon snack, 30% for dinner, 8% for an evening snack, and 30% for breakfast before the fMRI studies.

FMRI Tastant Solution Delivery

The paradigm was based on a task developed by our group (2, 3). Water and sucrose solutions were delivered with a programmable syringe pump (J-Kem Scientific, St. Louis MO). Two sterile silicone tubes were placed securely on the center of the tongue immediately adjacent to each other. Participants received 1.0 cc of 10% sucrose solution or ionic water. The paradigm

consists of four blocks of 20 trials each. Within blocks, sucrose and ionic water were presented pseudorandomly, every 20 seconds, for a total of 40 stimulus presentations per tastant.

MRI Protocol

Functional images were acquired in a sagittal plane using T2* weighted echo planar imaging (EPI) with an 8-channel head coil. Imaging data were collected on one of two scanners: a 3T GE Signa HDx (GE Medical Systems, Milwaukee, WI) (TR = 2000 ms, TE = 30 ms, flip angle = 80°, 64 x 64 matrix, ASSET factor = 2, 40 2.6-mm ascending interleaved axial slices with a 0.4-mm gap, 256 volumes) or, due to scanner upgrade, a 3T GE Discovery MR 750 (GE Medical Systems, Milwaukee, WI) (TR = 2000 ms, TE = 30 ms, flip angle = 80°, 64 x 64 matrix, ASSET factor = 2, 40 3.0-mm ascending interleaved axial slices, 256 volumes). The gradients system and application were not changed during the upgrade, and all post processing and analysis steps were consistent across datasets. Multisite imaging studies suggest that inter-participant variance far outweighs that of site or magnet variance (4-6). However, to control for potential differences due to magnet hardware, groups were balanced across magnets (Main text Table 1), each participant was scanned on the same scanner model for both imaging visits, and subject was nested within scanner and treated as random effect in subsequent analyses (7). The first four volumes of each run were discarded to discount T1 saturation. EPI-based field maps were also acquired to correct for susceptibility-induced geometric distortions. High-resolution T1-weighted FSPGR anatomical images (Signa HDx: TR=7.7 ms, TE=2.98 ms, flip angle=8°, 192x256 matrix, 172 1.2 mm sagittal slices; MR 750: TR=8.1 ms, TE=3.17 ms, flip angle=8°, 192×256 matrix, 172 1.2 mm sagittal slices) were obtained for subsequent spatial normalization and activation localization.

MRI Preprocessing

Functional images were preprocessed and analyzed using Analysis of Functional NeuroImages (AFNI) software, (8) and group analyses were performed using the nlme package in R (http://www.r-project.org). EPI images were motion-corrected and aligned to high-resolution anatomical images with align_epi_anat.py. Outliers were generated using AFNI's 3dToutcount. Volumes with more than 10% of the voxels marked as outliers were censored from subsequent analyses. Approximately 5.1% of volumes were censored (for all subjects: M = 13 volumes; SD = 9.1; range = 3-27). Registration to the MNI-152 atlas was performed using FMRIB's Non-linear Image Registration Tool (FNIRT), part of FSL (http://fsl.fmrib.ox.ac.uk/fsl/). The modeled hemodynamic responses were subsequently scaled so that beta weights would be equivalent to percent signal change (PSC). Data were smoothed to 6 mm FWHM using AFNI's 3dBlurToFWHM.

Assessments

Current symptoms were assessed using the State-Trait Anxiety Inventory (9), the Temperament and Character Inventory (10), the Beck Depression Inventory (11), and the Eating Disorders Inventory (12). *DSM-IV* diagnosis was made using either the Structured Clinical Interview for *DSM-IV* Axis I Disorders (SCID-I (13): 9 remitted anorexia nervosa [RAN], 7 control women [CW]) or the Mini International Neuropsychiatric Interview (M.I.N.I. (14): 16 RAN, 15 CW). One CW completed only Module H of the SCID. The M.I.N.I. has been validated against the much longer Structured Clinical Interview for DSM Disorders (SCID-P) and is a more time-efficient alternative to the SCID-P (14). Blood samples were drawn at 1:30 pm on the day prior to the first scan to measure baseline levels of estradiol in order to confirm participants were in the follicular phase of their menstrual cycle. Samples were not collected for 6 CW and 4 RAN. Participants also completed Likert scales rating anxiety and hunger ranging from 0 (not at all) to

7 (extreme) at 3:00 pm the day before a scan visit (baseline), and at 6:45 am (awakening), 8:45 am (pre-scan), and 11:00 am (post-scan) the day of a scan visit.

Delineation of Search Region of Interest

ROIs were based on previous studies that demonstrated altered limbic, striatal, and insula function during taste stimulation in eating disorders (see Figure S1) (3, 15-17). The structural connectivity of this circuitry in primates has been described in detail by Fudge and colleagues (18), who used retrograde and anterograde tract tracing techniques to determine the extent to which specific subdivisions of the insula influence the caudal ventral striatum in the primate. The anterior insula, which integrates sensory and amygdaloid inputs, projects to the classic ventral striatum. The agranular insula, the posteromedial agranular, lateral agranular, and posterolateral agranular subdivisions have the strongest ventral striatal inputs, and mediate olfactory, gustatory, and visceral information processing (19). The ventral striatum mediates goal-directed behaviors based, in part, on inputs from the amygdala. However, striatal areas caudal to the ventral striatum also receive inputs from the amygdala. In primates, the amygdala projects to the central ventral putamen, lateral amygdalostriatal area, and caudal ventral putamen, suggesting that these regions are also “limbic-related.” Caudal ventral striatal areas that receive amygdaloid inputs also receive significant innervation by agranular and dysgranular insula subdivisions that are themselves connected with the amygdala. This suggest that highly processed visceral/autonomic information, taste, and olfaction influence behavioral responses mediated by the caudal ventral striatum.

To improve power and reduce an inflated false discovery rate (20) primary analyses were restricted to a single gustatory-reward circuit mask (15) (Figure S1). Striatal ROIs were based upon known functional distinctions (21, 22), and included the bilateral ventral striatum (comprising the nucleus accumbens extending into the rostroventral caudate and ventrolateral

putamen), bilateral dorsal caudate, and the bilateral putamen. The bilateral insula and bilateral amygdala masks from the Harvard-Oxford atlas were used in their entirety. The five bilateral masks were merged into a single mask for use with ROI-based analyses.

Task-Based Connectivity Analysis

There are two recommended approaches for identifying seed regions for generalized psychophysiological interaction (gPPI) analyses. For an anatomical approach, the seed is based upon a region of interest that has been identified previously in the literature for the condition of interest. The second approach identifies a functionally relevant seed region – that is, one or more statistically significant activation clusters – across the entire study sample and relevant to the task condition of interest. Given the paucity of research focused on effects of hunger and satiety during taste activation, we chose to employ the second approach. This data-driven approach also avoids circularity by accounting for the main effect of the task condition but isolating effects distinct from the condition itself (23, 24). Seed regions were thus identified as follows: First, we performed an LME to examine the main effect of condition while controlling for taste, collapsed across groups. The time course of the BOLD signal for each participant was extracted from 6-mm spheres around the peak coordinates of the main effect of Condition using the same search region as our task-based activation analyses (voxel-wise $p<0.001$, $\alpha=0.05$). For each seed, time course activity was then detrended to remove global effects and fit to a gamma function. Seeds were convolved with each Condition vector (i.e., sucrose bolus when hungry, sucrose bolus when fed, water bolus when hungry, water bolus when fed) to create seed interaction regressors. A generalized linear model for each seed was created which included the original task and nuisance (e.g., motion) regressors, the four seed interaction regressors, and the seed time series. Single subject beta weights for each of the four seed interaction regressors were then used for group level analyses to identify other voxels showing a similar temporal pattern as seen in the seed regions. To examine the effect of the hungry and

fed state on group differences in functional connectivity strength in response to tastants, we used the same Group x Condition + tastants LME as described above and the same taste circuit search region mask (voxel-wise $p<0.001$, $\alpha=0.05$). The generalized psychophysiological interaction (gPPI) approach has been shown to have good sensitivity and specificity when tasks involve multiple conditions (23).

Supplemental Results

To evaluate potential group differences in tastant pleasantness rated at post-scan, we conducted a Group x Condition (hungry, fed) x Tastant (sucrose, water) linear mixed effects model, with subject included as random effect. There was a main effect of Tastant, $F(1,135)=25.16$, $p<0.001$. Overall, participants rated water as more pleasant than the sucrose solution, $t(134)=6.27$, $p<0.001$. No other main effects or interactions were statistically significant (all *p*s>0.12; Figure S2).

Task-Based ROI Sensitivity Analysis

To examine impact of AN subtype (e.g., restricting only vs those who also engaged in purging behaviors) and past diagnosis of major mood disorder (MDD) or anxiety disorder (including any lifetime diagnosis of an anxiety disorder or obsessive compulsive disorder) on results, we conducted a within-group RAN Visit + tastant LME analysis that included past subtype, history of MDD, and history of anxiety as covariates. There were no significant main effects of past subtype, MDD, or anxiety. Within the RAN group, there was a similar main effect of condition (hungry<fed) within the bilateral posterior putamen and the left insula, further suggesting that subtype and past comorbidities did not contribute significantly to the overall effect.

Exploratory Voxel-Wise Analyses. Whole-brain results were consistent with ROI findings, with additional clusters showing either a main effect of Condition (Table S2) or a Group x Condition

interaction (Table S2) in thalamic, medial prefrontal and parietal regions. In general, significant clusters consistently indicated that CW responded more strongly to tastants when hungry than when fed, whereas RAN responded less strongly to tastants when hungry than when fed. In whole-brain analyses a main effect of Condition was found in the left precuneus, paracentral lobule, ventral striatum, and rectal gyrus, as well as the right superior frontal gyrus (Table S2). In all regions, *post-hoc* analyses suggested both groups exhibited a stronger response to tastants when hungry relative to when fed. A Group x Condition interaction was also detected in multiple regions (Table S2) and tended to be in regions associated with attention or motor response. In general, significant clusters consistently indicated that CW responded to tastants more strongly when hungry, whereas RAN responded to tastants more strongly when fed. Several clusters, including the left precuneus, left postcentral gyrus, left supplementary motor area and right superior frontal gyrus also showed that CW had greater BOLD activation relative to RAN when hungry. Other clusters, including right postcentral gyrus, left precuneus, and left paracentral lobule, suggested that RAN had greater BOLD activation relative to CW when fed.

Task-Based Connectivity Analysis

Main effects of condition across all participants indicated that connectivity between the right ventral caudal putamen and left ventral caudal putamen, bilateral dorsal rostral putamen, and right ventral middle putamen was stronger during the hungry compared to fed state (Table S4). Similarly, connectivity between the right dorsal mid-insula and bilateral ventral middle putamen, left ventral caudal putamen, left amygdala, and left hippocampus was stronger during the hungry compared to fed state (Table S4).

Supplemental Figures

FIGURE S1. Illustration of gustatory and motivation regions of interest, which included the bilateral insula, amygdala, ventral striatum, dorsal caudate, and putamen.

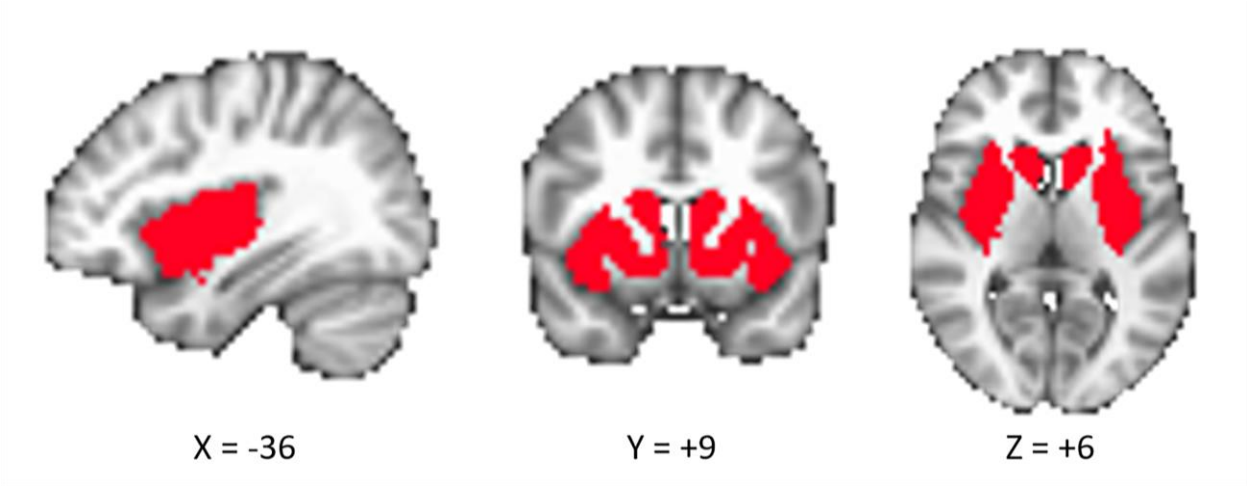

FIGURE S2. Graphs reflecting post-scan tastant pleasantness ratings for a main effect of Tastant [$F(1,135) = 25.16$, $p<0.001$], indicating that participants rated water as more pleasant than the sucrose solution. Error bars represent the standard error. R: right; CW: healthy control women; RAN: women remitted from anorexia nervosa.

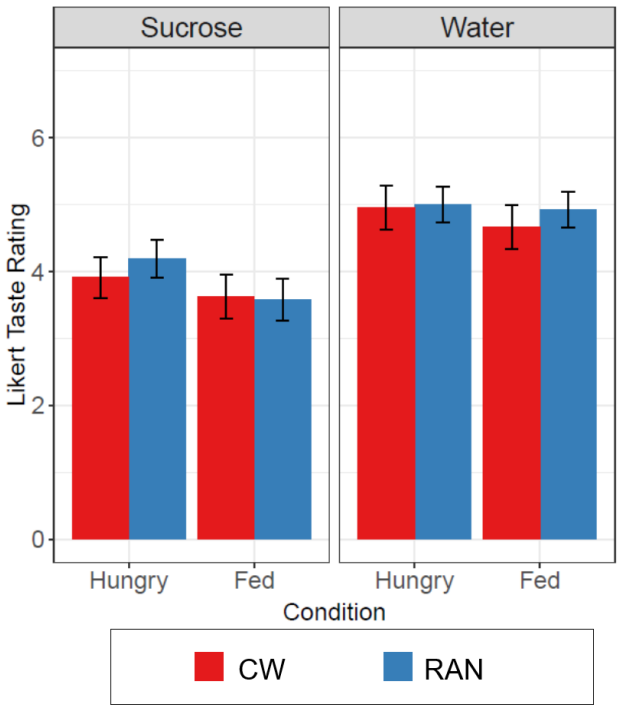

FIGURE S3. Graphs and image reflecting BOLD findings for a main effect of Condition [F(1,141) = 19.29, p=0.001] in the left ventral striatum (peak coordinates: x=-21, y=+9, z=-9). Error bars represent the standard error. R: right; CW: healthy control women; RAN: women remitted from anorexia nervosa. **p<0.01.

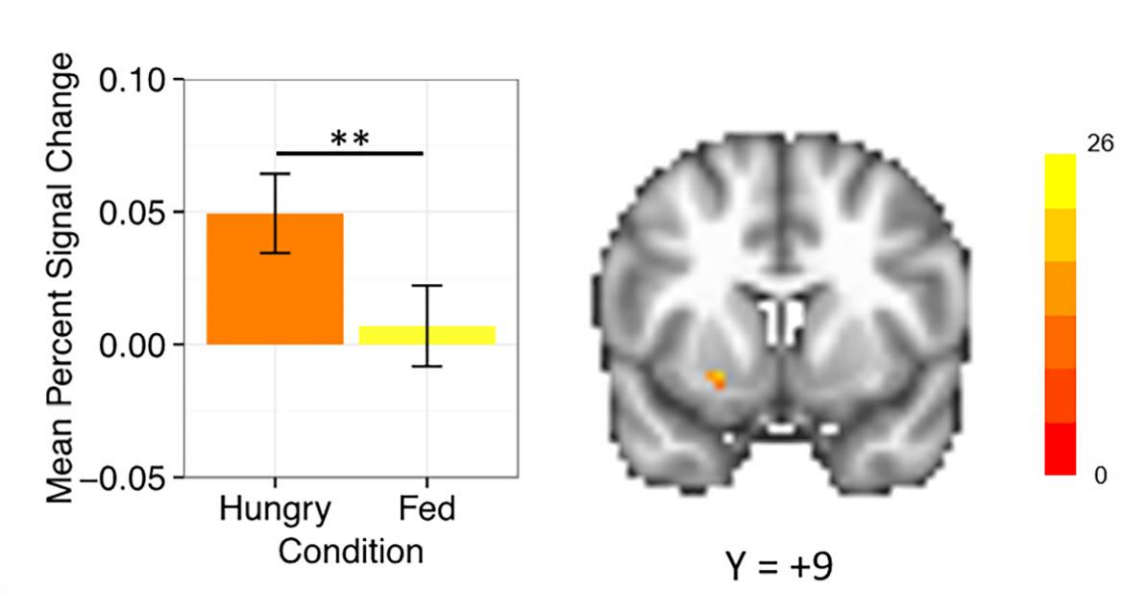

FIGURE S4. Linear mixed effect results demonstrating an interaction of Group (CW, RAN) by Condition (Hungry, Fed) in response to tastants (sucrose and water combined) within the left anterior insula (peak coordinates: x=-33, y=+9, z=+6), using a voxel-wise threshold of p<0.01 and a clusterwise threshold of α<0.05. CW: healthy control women; RAN: women remitted from anorexia nervosa; †p<0.1; *p<0.05; **p<0.01; ***p<0.001.

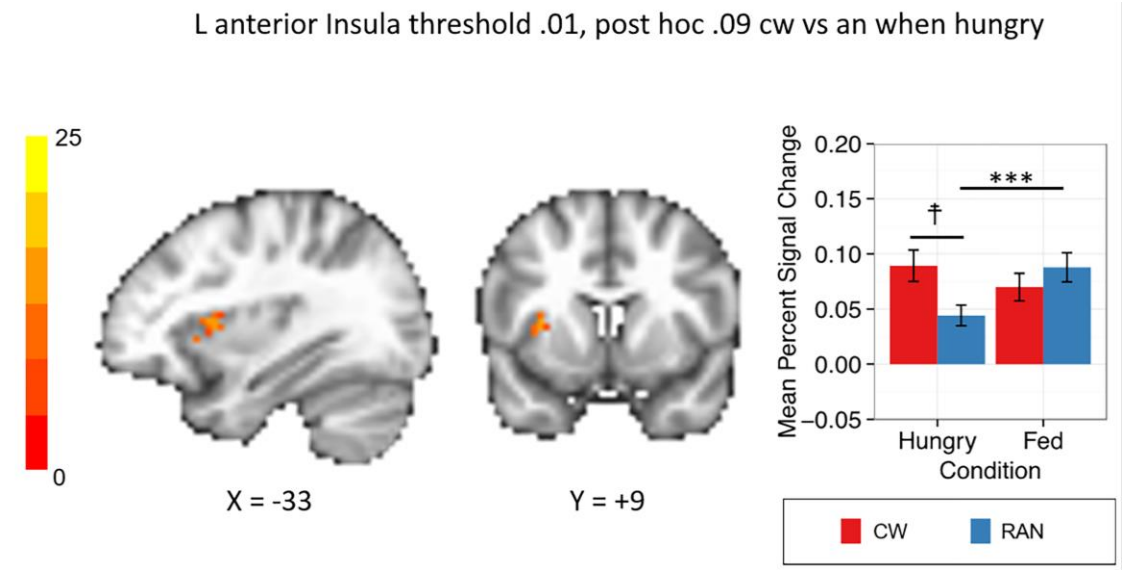

Supplemental Tables

TABLE S1. Study Schedule

	DAY 1 Intake and Assessments	DAY 2 Fasting/Fed Begin	DAY 3 Fasting/Fed Begin	DAY 4 Departure
6:00 am		Subject rise at 6:00 am	● Subject rise at 6:00 am ● 6:30 am Blood draw ● 6:45 am Interval assessments	● Subject rise at 6:00 am ● 6:30 am Blood draw ● 6:45 am Interval assessments
7:00 am		7:00-7:30 am Breakfast	● 7:00-7:30 am Breakfast at CTRI (if fed) ● 7:30 am Leave CTRI	● 7:00-7:30 am Breakfast at CTRI (if fed) ● 7:30 am Leave CTRI
8:00 am		● 8:00 am -12:00 pm Assessments	● Arrive at Keck MR Center ● Pre-scan questionnaires	● Arrive at Keck MR Center ● Pre scan questionnaires
9:00 am			● 9:00-10:30 am fMRI scan	● 9 :00-10:30 am fMRI scan
10:00 am			● Post scan questionnaires ● Return to CTRI	● Post scan questionnaires ● Return to CTRI
11:00 am		● 11:30 am Lunch at CTRI	● 11:30 Lunch at CTRI ● End of Day A (fast or fed)	● 11:30 am Lunch at CTRI ● End of Day B (fast or fed)
12:00 pm		● 12:00 pm Begin Day A (16-hr fast or fed) ● Interval assessments	● 12:00 Begin Day B (16-hr fast or fed) ● Interval assessments	End of study; Discharge
1:00 pm	● Subject arrival at CTRI ● 1:00-2:45 pm Intake and medical evaluation ● 2:45 pm Snack:			
2:00 pm		*2:45 pm Snack*	*2:45 pm Snack*	
3:00 pm	Cognitive assessments	Interval assessments	Interval assessments	
4:00 pm				
5:00 pm	Dinner	*Dinner*	*Dinner*	
6:00 pm		Interval assessments	Interval assessments	
7:00 pm	Assessments			
8:00 pm				
9:00 pm	Snack	● Interval assessments ● *Snack (8:45-9:00 pm fed day only)*	● Interval assessments ● *Snack (8:45-9:00 pm fed day only)*	
10:00 pm	Subject bedtime	Bedtime Interval assessments	Bedtime Interval assessments	

The night before the hungry day (16 hour fast) subjects did not consume anything besides water after dinner at 5:00 pm, had no breakfast, and were scanned at 9:00 am the next day. The night before the fed day, subjects had dinner at 5:00 pm, a snack at 8:45 pm and then breakfast at 7:00 am before the 9:00 am scan.

TABLE S2. Exploratory Whole-brain linear mixed effects results demonstrating a main effect of Condition (Hungry, Fed) and a Group (CW, RAN) x Condition (Hungry, Fed) interaction in response to tastants (sucrose and water combined)

		Main Effect of Condition					Post-Hoc Comparisons		
Region	**Volume (voxels)**	**x**	**y**	**z**	***F***	η^2	**Contrast**	***t* ratio**	***p***
L Precuneus	39	-12	-60	72	23.15	0.069	Hungry > Fed	3.269	0.001
L Paracentral Lobule	28	-9	-33	72	25.33	0.073	Hungry > Fed	3.249	0.001
L Paracentral Lobule	21	-3	-12	72	24.95	0.031	Hungry > Fed	3.304	0.001
L Ventral Middle Putamen	18	-21	9	-9	19.25	0.054	Hungry > Fed	3.175	0.002
R Superior Frontal Gyrus	18	24	-6	63	21.17	0.047	Hungry > Fed	2.748	0.007
L Rectal Gyrus	14	-6	57	-18	27.85	0.122	Hungry > Fed	4.707	<0.001
		Group x Condition Interaction					**Post-Hoc Comparisons**		
Region	**Volume (voxels)**	**x**	**y**	**z**	***F***	η^2	**Contrast**	***t* ratio**	***p***
R Postcentral Gyrus	62	63	-6	36	27.49	0.088	**CW:** Hungry > Fed	3.824	<0.001
							RAN: Fed > Hungry	4.068	<0.001
							Fed: RAN > CW	3.063	0.005
L Precuneus	44	-3	-48	72	27.36	0.056	**CW:** Hungry > Fed	4.653	<0.001
							RAN: Fed > Hungry	2.583	0.022
							Fed: RAN > CW	1.832	0.088
							Hungry: CW > RAN	1.744	0.088
L Paracentral Lobule	32	-9	-21	72	21.29	0.050	**CW:** Hungry > Fed	5.493	<0.001
							RAN: Fed > Hungry	2.111	0.049
							Fed: RAN > CW	2.186	0.049
L Cuneus	27	-18	-63	33	22.32	0.036	**CW:** Hungry > Fed	4.205	<0.001
							RAN: Fed > Hungry	3.353	0.002
L Precentral Gyrus	25	-54	-3	33	25.01	0.037	**CW:** Hungry > Fed	3.462	0.003
							RAN: Fed > Hungry	3.119	0.004
							Fed: RAN > CW	1.775	0.110

L Postcentral Gyrus	21	-66	-21	30	18.62	0.072	**CW:** Hungry > Fed	2.729	0.013
							RAN: Fed > Hungry	4.646	<0.001
							Hungry: CW > RAN	2.695	0.013
L Ventral Caudal Putamen	20	-27	-9	0	25.39	0.056	**CW:** Hungry > Fed	2.693	0.016
							RAN: Fed > Hungry	4.250	<0.001
							Hungry: CW > RAN	2.122	0.052
R Thalamus	20	12	-18	15	16.57	0.033	**CW:** Hungry > Fed	2.457	0.030
							RAN: Fed > Hungry	3.627	0.002
							Fed: RAN > CW	1.705	0.127
L Supplementary Motor Area	20	-3	-3	48	17.67	0.044	**CW:** Hungry > Fed	3.328	0.004
							RAN: Fed > Hungry	2.872	0.009
							Hungry: CW > RAN	1.847	0.095
R Superior Frontal Gyrus	19	27	-3	63	19.08	0.053	**CW:** Hungry > Fed	4.108	<0.001
							RAN: Fed > Hungry	2.900	0.009
							Hungry: CW > RAN	2.058	0.060
R Postcentral Gyrus	18	39	-18	33	19.99	0.044	**CW:** Hungry > Fed	3.240	0.003
							RAN: Fed > Hungry	4.169	<0.001
							Hungry: CW > RAN	1.763	0.113
L Postcentral Gyrus	16	-51	-18	33	30.75	0.057	**CW:** Hungry > Fed	4.066	<0.001
							RAN: Fed > Hungry	2.999	0.006
							Hungry: CW > RAN	2.103	0.055

Coordinates are reported for the peak voxel. L: left; R: right; CW: healthy comparison women; RAN: women remitted from anorexia nervosa. Intrinsic smoothness was estimated using the spatial autocorrelation function (acf) option in AFNI's 3dFWHMx. Minimum cluster sizes were calculated with AFNI's 3dClustSim to guard against false positives. The required minimum cluster size was 378 µL (14 contiguous voxels) at the whole brain level. Post hoc analyses were performed using lsmeans in R and false discovery rate corrected to control for multiple tests.

TABLE S3. Results of the Group (CW, RAN) by Condition (Hungry, Fed) LME in response to tastants (sucrose and water combined) within the taste circuit search region of interest

A.

Main Effect of Condition							Post-Hoc Comparisons		
Region	**Volume (voxels)**	**x**	**y**	**z**	***F***	***η²***	**Contrast**	***t* ratio**	***p***
L Ventral Striatum	12	-21	9	-9	19.29	0.056	Hungry > Fed	3.317	<0.001
Group x Condition Interaction							**Post-Hoc Comparisons**		
Region	**Volume (voxels)**	**x**	**y**	**z**	***F***	***η²***	**Contrast**	***t* ratio**	***P***
L Ventral Caudal Putamen	8	-30	-15	0	18.81	0.045	**CW:** Hungry > Fed	2.382	0.037
							RAN: Fed > Hungry	3.707	0.001
							Hungry: CW > RAN	2.068	0.059
L Ventral Caudal Putamen	7	-27	-9	0	25.39	0.060	**CW:** Hungry > Fed	2.687	0.016
							RAN: Fed > Hungry	3.916	<0.001
							Hungry: CW > RAN	2.297	0.035

B.

Group x Condition Interaction							Post-Hoc Comparisons		
Region	**Volume (voxels)**	**x**	**y**	**z**	***F***	***η²***	**Contrast**	***t* ratio**	***P***
L Ventral Caudal Putamen	33	-27	-9	0	25.39	0.050	**CW:** Hungry > Fed	2.532	0.025
							RAN: Fed > Hungry	3.658	0.001
							Hungry: CW > RAN	2.226	0.041
L Anterior Insula	21	-33	9	6	15.13	0.050	**RAN:** Fed > Hungry	3.858	0.001
							Hungry: CW > RAN	2.061	0.090
L Ventral Middle Putamen	15	-21	3	-6	11.95	0.045	**CW:** Hungry > Fed	4.245	<0.001

Section A indicates clusters corresponding to a voxel-wise probability of $p<0.001$ and a clusterwise probability of $\alpha<0.05$ (two-sided) to correct for multiple comparisons. Section B indicates additional clusters corresponding to a relaxed voxel-wise probability of $p<0.01$ and a clusterwise probability of $\alpha<0.05$ (two-sided) to correct for multiple comparisons. Coordinates are reported for the peak activation. L: left; R: right; CW: healthy control women; RAN: women remitted from anorexia nervosa. Intrinsic smoothness was estimated using the spatial autocorrelation function (acf) option in AFNI's 3dFWHMx. Minimum cluster sizes were calculated with AFNI's 3dClustSim to guard against false positives. The required minimum cluster size was 135 µL (5 contiguous voxels) at the ROI level. Post hoc analyses were performed using lsmeans in R and false discovery rate corrected to control for multiple tests.

TABLE S4. Main effect of Condition (Hungry, Fed) and Group (RAN, CW) x Condition (Hungry, Fed) interactions in functional connectivity to tastants (sucrose and water combined) within the taste circuit search region of interest ($p < 0.001$, $\alpha < 0.05$)

		Main Effect of Condition					Post-Hoc Comparisons		
Region	**Volume (voxels)**	**x**	**y**	**z**	***F***	***η²***	**Contrast**	***t* ratio**	***p***
Right Dorsal Mid-Insula Seed									
L Ventral Middle Putamen	25	-21	12	-9	29.82	0.035	Hungry > Fed	3.111	0.002
L Ventral Caudal Putamen	5	-30	-15	0	19.41	0.070	n.s.		
R Ventral Middle Putamen	6	21	9	-9	21.86	0.036	Hungry > Fed	2.203	0.029
L Amygdala	7	-21	0	-21	20.23	0.027	Hungry > Fed	3.837	<0.001
L Hippocampus	5	-15	-6	-15	17.3	0.026	n.s.		
Right Ventral Caudal Putamen Seed									
L Ventral Caudal Putamen	60	-30	-15	0	31.85	0.120	Hungry > Fed	5.164	<0.001
L Dorsal Rostral Putamen	13	-30	9	6	19.49	0.066	Hungry > Fed	4.058	<0.001
R Ventral Middle Putamen	10	21	9	-9	29.48	0.045	Hungry > Fed	3.968	<0.001
R Dorsal Rostral Putamen	8	27	9	6	20.74	0.043	Hungry > Fed	1.743	0.084
		Group x Condition Interactions					**Post-Hoc Comparisons**		
Region	**Volume (voxels)**	**x**	**y**	**z**	***F***	***η²***	**Contrast**	***t* ratio**	***p***
Right Dorsal Mid-Insula Seed									
L Ventral Caudal Putamen	31	-30	-15	0	31.19	0.076	**CW:** Hungry > Fed	4.53	<0.001
							RAN: Fed > Hungry	3.53	0.001
							Hungry: CW > RAN	2.65	0.015
	8	-21	3	-9	16.14	0.024	**CW:** Hungry > Fed	3.45	0.003
R Dorsal Rostral Putamen	6	27	9	6	17.25	0.035	**CW:** Hungry > Fed	2.58	0.024
							RAN: Fed > Hungry	2.54	0.024
							Hungry: CW > RAN	1.85	0.095
L Anterior Insula	6	-33	9	6	21.4	0.024	**CW:** Hungry > Fed	2.15	0.066

							RAN: Fed > Hungry	3.95	<0.001
Right Ventral Caudal Putamen Seed									
L Ventral Caudal Putamen	25	-30	-15	0	30.04	0.114	**CW:** Hungry > Fed	6.07	<0.001
							RAN: Fed > Hungry	2.14	0.045
							Hungry: CW > RAN	3.50	0.002
R Dorsal Rostral Putamen	6	27	6	6	19.44	0.047	**CW:** Hungry > Fed	3.74	0.001
							RAN: Fed > Hungry	1.75	0.109
							Hungry: CW > RAN	2.17	0.070
R Parahippocampal Gyrus/Amygdala	5	27	-3	-27	14.37	0.049	**CW:** Hungry > Fed	2.22	0.115

Coordinates are reported for the peak voxel. L: left; R: right. CW: healthy control women; RAN: women remitted from anorexia nervosa. Minimum cluster sizes were calculated with AFNI's 3dClustSim to guard against false positives. The required minimum cluster size was 135 µL (5 contiguous voxels) at the ROI level. Post hoc analyses were performed using lsmeans in R and false discovery rate corrected to control for multiple tests.

REFERENCES

1. Gautier J, Del Parigi A, Chen K, et al. Effect of satiation on brain activity in obese and lean women. Obesity Research. 2001;9(11):676-84.
2. Oberndorfer T, Frank G, Fudge J, et al. Altered insula response to sweet taste processing after recovery from anorexia and bulimia nervosa. Am J Psychiatry. 2013;214(2):132-41.
3. Wagner A, Aizenstein H, Frank GK, et al. Altered insula response to a taste stimulus in individuals recovered from restricting-type anorexia nervosa. Neuropsychopharmacology. 2008;33(3):513-23.
4. Gountouna V-E, Job D, McIntosh A, et al. Functional Magnetic Resonance Imaging (fMRI) reproducibility and variance components across visits and scanning sites with a finger tapping task. Neuroimage. 2010;49(1):552-60.
5. Suckling J, Ohlssen D, Andrew C, et al. Components of variance in a multicentre functional MRI study and implications for calculation of statistical power. Hum Brain Mapp. 2008;29(10):1111-22.
6. Brown G, Mathalon D, Stern H, et al. Multisite reliability of cognitive BOLD data. Neuroimage. 2011;54(3):2163-75.
7. Glover G, Mueller B, Turner J, et al. Function biomedical informatics research network recommendations for prospective multicenter functional MRI studies. J Magn Reson Imaging. 2012;36(1):39-54.
8. Cox R. AFNI: software for analysis and visualization of functional magnetic resonance neuroimages. Comput Biomed Res. 1996;29:162-73.
9. Spielberger C, Gorsuch R, Lushene R. STAI Manual for the State Trait Anxiety Inventory. Palo Alto, CA: Consulting Psychologists Press; 1970.
10. Cloninger C, Przybeck T, Svrakic D, et al. The Temperament and Character Inventory (TCI): A guide to its development and use. 2, Chapter 4. St. Louis MO, Center for Psychobiology of Personality, Washington University, ISBN 0-9642917-1-1 1994. p. 19-28.
11. Beck AT, Ward M, Mendelson M, et al. An Inventory for measuring depression. Arch Gen Psychiatry. 1961;4:561-71.
12. Garner DM. Eating Disorder Inventory-2 Professional Manual. Odessa FL: Psychological Assessment Resources, Inc.; 1991 1990.
13. First M, Biggon M, Spitzer R, et al. User's guide for the structured clinical interview for DSM-IV Axis II personal disorders (SCID-II). American Psychiatric Press, Washington DC. 1997.

14. Sheehan DV, Lecrubier Y, Sheehan KH, et al. The Mini-International Neuropspychiatric Interview (M.I.N.I.): the development and validation of a structured diagnostic psychiatric interview for DSM-IV and ICD-10. J Clin Psychiatry. 1998;59(20):22-33;quiz 4-57.
15. Ely A, Wierenga C, Bischoff-Grethe A, et al. Response in taste circuitry is not modulated by hunger and satiety in women remitted from bulimia nervosa. J Abnorm Psychol. 2017;126(5):519-30.
16. Frank G, Bailer UF, Henry S, et al. Increased dopamine D2/D3 receptor binding after recovery from anorexia nervosa measured by positron emission tomography and [^{11}C]raclopride. Biological Psychiatry. 2005;58(11):908-12.
17. Oberndorfer T, Simmons A, McCurdy D, et al. Greater anterior insula activation during anticipation of food images in women recovered from anorexia nervosa versus controls. Psychiatry Res. 2013 214(2):132-41.
18. Fudge J, Breibart M, Danish M, et al. Insular and gustatory inputs to the caudal ventral striatum in primates. J Comp Neurol. 2005;490(2):101-18.
19. Carmichael S, Price J. Sensory and premotor connections of the orbital and medial prefrontal cortex of macaque monkeys. J Comp Neurol. 1995;363(4):642-64.
20. Poldrack R, Baker C, Durnez J, et al. Scanning the horizon: towards transparent and reproducible neuroimaging research. Nat Rev Neurosci. 2017;18(2):115-26.
21. Martinez D, Slifstein M, Broft A, et al. Imaging human mesolimbic dopamine transmission with positron emission tomography. Part II: amphetamine-induced dopamine release in the functional subdivisions of the striatum. J Cereb Blood Flow Metab. 2003;23(3):285-300.
22. Mawlawi O, Martinez D, Slifstein M, et al. Imaging human mesolimbic dopamine transmission with positron emission tomography: I. Accuracy and precision of D(2) receptor parameter measurements in ventral striatum. J Cereb Blood Flow Metab. 2001;21(9):1034-57.
23. McLaren DRM, Xu G, Johnson S. A generalized form of context-dependent psychophysiological interactions (gPPI): a comparison to standard approaches. Neuroimage. 2012;61(14):1277-86.
24. Harrison T, McLaren D, Moody T, et al. Generalized psychophysiological interaction (PPI) analysis of memory related connectivity in individuals at genetic risk for Alzheimer's Disease. J Vis Exp. 2017;14:129.